# ASSESSMENT OF HYDROGEN FLAME LENGTH AFTER FULL BORE PIPELINE RUPTURE

**Makarov, D.V., Molkov, V.V.**

**HySAFER Centre, Ulster University, Shore Road, Newtownabbey, Co. Antrim, BT37 0QB, UK, dv.makarov@ulster.ac.uk, v. molkov@ulster.ac.uk**

## ABSTRACT

The study aims at the development of a safety engineering methodology for the assessment of flame length after full-bore rupture of hydrogen pipeline. The methodology is validated using experimental data on hydrogen jet flame from full-bore pipeline rupture by Acton et al. (2010). The experimental pressure dynamics in the hydrogen pipeline system is simulated using previously developed adiabatic and "isothermal" blowdown models. The hydrogen release area is taken as equal, similar to the experiment, to doubled pipeline cross-section as hydrogen was coming out from both sides of the ruptured pipe. The agreement with the experimental pressure decay in the piping system was achieved using discharge coefficient $C_D$=0.26 and $C_D$=0.21 for adiabatic and "isothermal" blowdown model respectively that indicates significant friction and minor pressure losses. The hydrogen flame length was calculated using the dimensionless correlation by Molkov and Saffers (2013). The correlation relies on the density of hydrogen in the choked flow at the pipe exit. The maximum experimental flame length between 92 m and 111 m was recorded at 6 s after the pipe rupture under the ground. The calculated by the dimensionless correlation flame length is 110 m and 120 m for the "isothermal" and adiabatic blowdown model respectively. This is an acceptable accuracy for such a large-scale experiment. It is concluded that the methodology can be applied as an engineering tool to assess flame length resulting from ruptured hydrogen pipelines.

## 1.0 INTRODUCTION

The use of pipelines for the transport of hydrogen in large quantities is a viable scenario of the emerging hydrogen economy. Statistics show that majority of hydrogen releases are ignited [1]. Knowledge of jet flame length in case of severe pipeline accident is one of the key parameters for carrying out hydrogen safety engineering. Recent studies [2,3] demonstrated that though jet flames are the subject of extensive research since 1949, the engineering methods for the assessment of jet flame length remain the focus of continuous scientific development. While the paper by Bradley and co-workers [3] develops the jet flame length correlation applicable to different fuels, the work by Molkov and Saffers [2] focuses on hydrogen flames only. The authors [2] argue that correlations built using Froude number alone are not suitable to describe the length of under-expanded jet flames. The developed universal flame length correlation depends on the dimensionless parameter $(\rho_N/\rho_a)(U_N/C_N)^3$ and capable to describe hydrogen flame length for buoyancy-controlled, momentum-dominated expanded and chocked under-expanded jets respectively:

$$\begin{cases} \frac{L_f}{D_N} = 1403\left[\left(\frac{\rho_N}{\rho_a}\right)\left(\frac{U_N}{C_N}\right)^3\right]^{0.196} & \text{for } \left(\frac{\rho_N}{\rho_a}\right)\left(\frac{U_N}{C_N}\right)^3 \le 0.0001, \\ \frac{L_f}{D_N} = 230 & \text{for } 0.0001 < \left(\frac{\rho_N}{\rho_a}\right)\left(\frac{U_N}{C_N}\right)^3 < 0.07, \\ \frac{L_f}{D_N} = 805\left[\left(\frac{\rho_N}{\rho_a}\right)\left(\frac{U_N}{C_N}\right)^3\right]^{0.47} & \text{for } \left(\frac{\rho_N}{\rho_a}\right)\left(\frac{U_N}{C_N}\right)^3 \ge 0.07. \end{cases} \quad (1)$$

where $L_f$ is the flame length, $D_N$ is the real nozzle diameter, $\rho_N$ is the hydrogen density in the nozzle, $\rho_a$ is the density of the surrounnding atmosphere, $U_N$ is the hydrogen velocity in the nozzle, $C_N$ is hydrogen speed of sound in the nozzle.

The non-dimensional parameter $(\rho_N/\rho_a)(U_N/C_N)^3$ explicitly containes Mach number $(U_N/C_N)$ and also may be rewritten in terms of Reynolds and Froude numbers as $(g \cdot \mu_N)/(\rho_S \cdot C_N^3)\, Re\, Fr$. The correlation is presented graphically in Fig.1. All three jet fire regimes are easily identifiable: for the parameter $(\rho_N/\rho_a)(U_N/C_N)^3 < 0.0001$ the jet fires are buoyant, in-between values 0.0001 and 0.07 they are expanded momentum-dominated jets, and above 0.07 the jets are under-expanded with chocked in the nozzle flow. The correlation (1) is conservative, i.e. all experimental points remain under the correlation line. It was validated for storage pressures up to 90 MPa, stored hydrogen temperature range 80-300 K, and leak diameters 0.4 – 51.7 mm. Use of the nozzle density $\rho_N$ and the nozzle velocity $U_N$ in the flame correlation Eq.(1) also implicitly accounts for pressure losses in hydrogen release line.

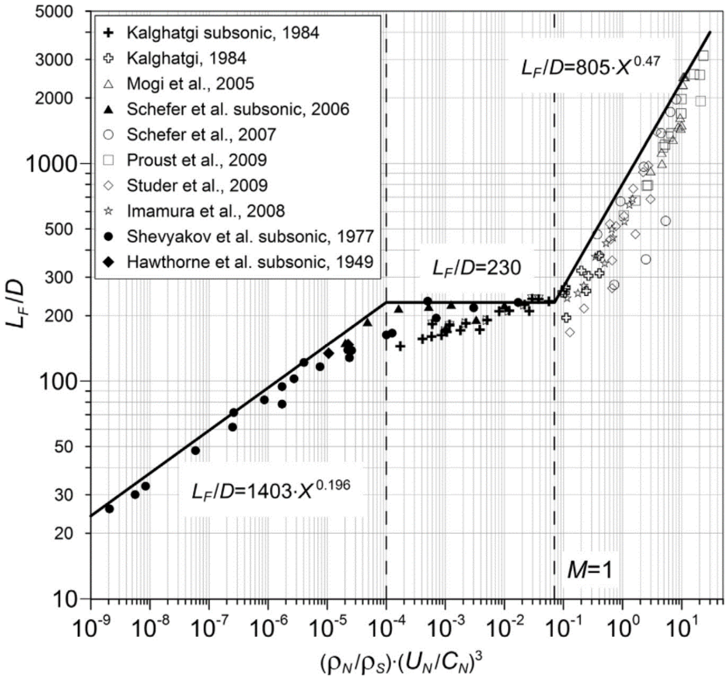

Figure 1. Dimensionless correlation for hydrogen jet flames [2].

The use of the correlation for practical engineering analysis of pipeline accidents is not straightforward:

- Flow from a ruptured pipeline is different from a jet flow used in validation experiments;
- Friction and minor losses are essential for pipe flow that is different to classical flow from an orifice in a storage vessel.

The paper aims to develop a methodology for the use of the correlation (1) for the assessment of hydrogen jet flames from ruptured pipelines.

## 2.0 VALIDATION EXPERIMENTS

Experiments were conducted on request of Air Products by GL Industrial Services UK at the GL Spadeadam test site (Cumbria, UK) and described in detail in [4].

Hydrogen was stored in a pipeline of 48” (1.22 m) diameter having a total volume of 163 $m^3$ at pressure 60 bar. The storage was consecutively connected via 12” (0.30 m) and 8” (0.20 m) diameter pipework and T-piece to the test section represented by a loop made of 6” (0.15 m) diameter pipeline. The total length of the 12” pipeline section was 3.5 m, the 8” pipe section length was 51 m and the total length of the 6” pipeline loop was 28 m.

The pipe section for rupture was buried in the centre of a specially prepared location where the soil was removed from an area of 6×6 m and a depth of 2 m. Two nearly identical large-scale hydrogen pipeline rupture experiments with fire were performed. In Test 1 the excavated volume was backfilled with fine soil, and in Test 2 the volume was filled with a mixture of sand and soil. The depth of cover above the pipeline was 1 m.

The buried loop section of the 6” pipe was intentionally failed using explosive charge creating hydrogen release from two open pipe ends and immediately igniting the hydrogen release. The explosive charge was positioned on 6” pipeline loop opposite of the T-junction and on the symmetry line so that distance from the rupture point to the T-junction connecting 6” pipeline loop to the 8” pipework is the same along any side of the loop. The explosive charge was designed to cut 85% of the pipe circumference at two locations 1.6 m from each other making sure the open pipe ends are still rigidly connected and not ejected from the trench. No special measures were taken to control the release. Hydrogen storage blowdown continued till the overpressure in the pipeline system became less than 0.5 bar when the experiment was terminated. The blowdown continued for about 80 s.

Before the commencement of the test programme, the hydrogen storage reservoir was purged with hydrogen. Gas sampling before the test showed that the residual methane concentration was below 0.02%. Both sides of the test loop were instrumented to measure static pressure at the pipe wall, stagnation pressure on the pipe centreline and temperature close to the release point. The mass flow rate during the experiment was not measured, however “the pipework either side of the test section was instrumented to measure the static pressure at the pipe wall, the stagnation pressure on the centreline of the pipe, and temperature of the flowing gas as it approached the release point” [4]. Ambient environment measurements included meteorological conditions, flame dimensions, incident radiation levels, maximum overpressure on pipe failure, gas release and ignition.

Experimentalists estimated the total mass of released hydrogen as 800 kg. Mass flow rate was calculated from measurements of total pressure, static pressure and temperature close to the release orifices. Peak mass flow rate was evaluated as 53.7 kg/s and decreased after 25 s of release to 9.8 kg/s. The experimentally measured flame length is given in Figure 2. The flame length was deduced from video records made from four locations around the test site and corrected for geometrical distortion. The experimental paper [4] reports that in the first test the maximum flame length varied between 91.6 m and 111.5 m, and in the second test the flame length varied between 62 and 88.4 m. According to the graphical material in [4], the maximum flame length of 92 m was reached in Test 1 at about 5 s, and in Test 2 the maximum flame length of 88 m was reached at about 6 s. The flame length subsided to about 20 m at 80 s from the release start.

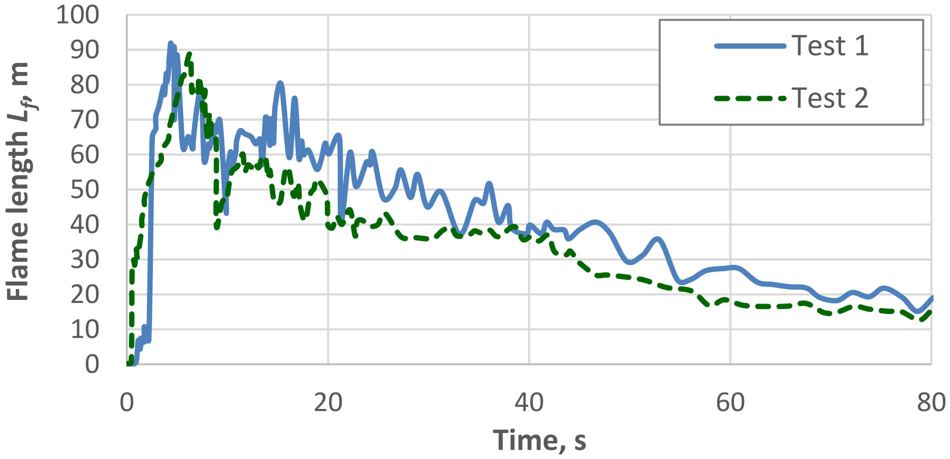

Figure 2. Experimental flame length dynamics [4].

High luminosity of the large-scale hydrogen flame was observed in the performed experiments. The fraction of energy released as radiation in both cases was estimated as 0.29, which is higher than for small-scale hydrogen flame laboratory experiments and similar to large-scale natural gas flames.

Experimentalists highlighted that flame length analysis was subject to uncertainties due to the nature of the experimental release arrangement (a large amount of generated steam and entrainment of backfill).

## 3.0 JET FLAME ASSESSMENT STRATEGY

### 3.1 Blowdown modelling

The analysis performed in this study relies on the use of fundamentally based and well-validated under-expanded jet theory [5,6] and blowdown model [5]. Both the under-expanded jet theory, describing properties of hydrogen as it flows from storage, and the blowdown model are realised as freely available engineering tools at the e-Laboratory developed within the NET-Tools project [7].

The e-Laboratory realises the blowdown model [5] in two options: adiabatic and “isothermal” release. The adiabatic release represents a limit of a very quick process where heat transfer does not have time to noticeably affect the release parameters. However, as in the experiment, the compressed hydrogen storage was organised in a 1.22 m diameter pipe, which has a rather developed surface area compared to a typical storage vessel. Hydrogen had to pass developed and thermally uninsulated pipework with a total length of 68.5 m, the heat transfer is expected to play a noticeable role in the blowdown process. The work by Schefer and co-workers [8] demonstrated that during 480 s long release from a 0.617 $m^3$ vessel the hydrogen temperature behaviour in the vessel was far from adiabatic – it initially dropped by about 50 degrees to -45°C, but then stabilised at -35°C, which was 40°C below initial temperature. To reflect this practical behaviour the “isothermal” blowdown model allows the temperature in the storage to drop following adiabatic solution until a specified limit, after which the temperature stays constant and equal to that limit (making the model effectively a combination of adiabatic and isothermal models).

The following initial parameters were used in simulations: storage volume 163 $m^3$, initial pressure 60 bar, initial temperature 283 K. This corresponds to the total hydrogen mass in the storage 806 kg (close to the experimentalists’ estimate of 800 kg, [4]). To achieve storage overpressure 0.5 bar at 80 s as described in [4] the outflow orifice diameter (in the assumption of discharge coefficient $C_D$=1) should be equal to 0.109 m with the adiabatic blowdown model, which corresponds to cross-section area $9.33 \cdot 10^{-3}$ $m^2$. In absence of information on the storage temperature in [4], the temperature limit in the “isothermal” solution was set to 40 degrees below the initial one, i.e. 243 K, similar to the observation in [8]. In this case, 0.5 bar overpressure at 80 s can be achieved with the orifice diameter 0.098 m ($C_D$=1) corresponding to outflow area $7.54 \cdot 10^{-3}$ $m^2$.

In both cases the outflow area is significantly smaller than the doubled cross-section area of the 6” pipe, $3.65 \cdot 10^{-2}$ $m^2$. The difference originates from the release conditions not complying with the original model assumption of release through an orifice (rather than through pipework) without pressure losses. The experimental release via a long pipe implies significant losses and pressure drop at the release point. The use of a smaller release orifice diameter instead of a detailed account of friction and minor losses was considered as an acceptable quick-fix for the described discrepancy between the model calculation scheme and the actual release. Decrease of outflow cross-section can be described using discharge coefficient $C_D$ that can be calculated for each of the blowdown models as follows:

- Adiabatic blowdown $C_{D_{ad}} = \frac{9.33 \cdot 10^{-3}}{3.65 \cdot 10^{-2}} = 0.255 \approx 0.26$,
- “Isothermal” blowdown $C_{D_{isotherm}} = \frac{7.54 \cdot 10^{-3}}{3.65 \cdot 10^{-2}} = 0.207 \approx 0.21$.

Simulated mass flow rate from the pipe and pressure dynamics are demonstrated in Fig.3 and Fig.4 respectively. The initial mass flow rate for the “isothermal” release is 28.0 kg/s, which is lower than that for adiabatic release, 34.7 kg/s. This is is due to the lower outflow area of the “isothermal” release.

Both simulated mass flow rates are somehow lower than the peak mass flow rate estimated by the experimentalists from pressure and temperature measurements in the pipe as 53.7 kg/s [4], which makes a 35% difference for the simulated adiabatic release and a 48% difference for the isothermal one. In the authors' view, this larger experimental mass flow rate corresponds to the emptying of the pipework near the release point right after the rupture and should decrease as soon as pressure gradients are established along the pipeline.

Experimentalists estimated that 25 s after the release start the mass flow rate subsided to 9.8 kg/s. Simulated values 25 s after the start of the release are 10.7 kg/s (9% difference) and 11.4 kg/s (14%) for adiabatic and "isothermal" releases respectively. This quite good agreement with the experimental pressure dynamics implicitly supports the suggestion above that the peak mass flow rate of 53.7 kg/s estimated in the experiment existed only during a very short period and the simulated blowdown dynamics is close to the one in the actual experiment during the most of the release period.

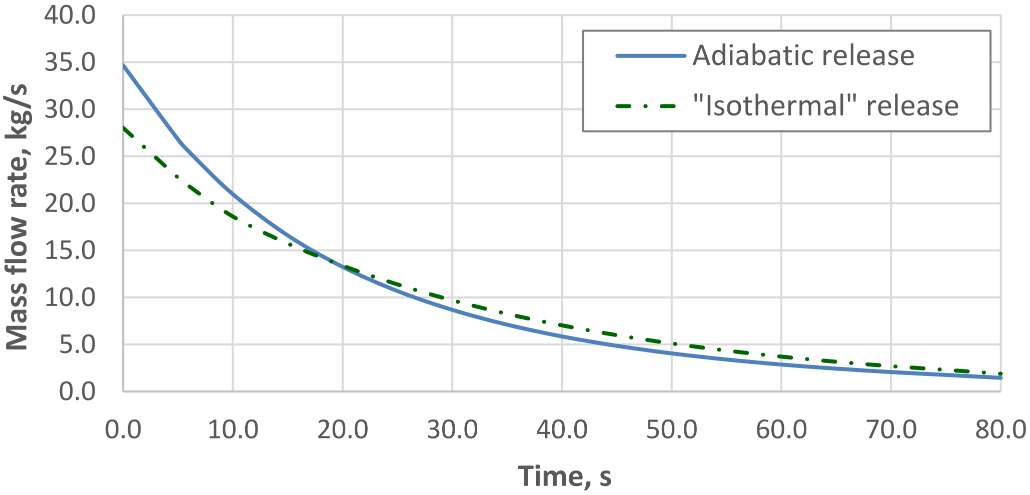

Figure 3. The simulated mass flow rate during hydrogen storage blowdown.

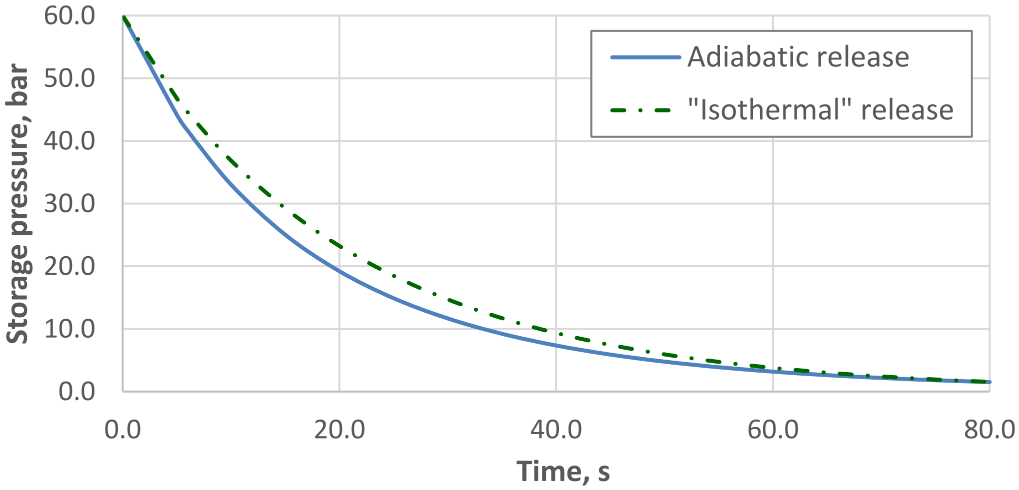

Figure 4. The simulated pressure dynamics in hydrogen pipeline during blowdown.

### 3.2 Flame length dynamics

The conservative dimensionless correlation (1) [2] is used for the calculation of hydrogen flame length dynamics during choked outflow conditions:

$$L_f = 805 \cdot [\rho_N/\rho_a]^{0.47} \cdot D_N, \qquad (2)$$

where the diameter of the opening found in the blowdown analysis was $D_{N_{ad}} = 0.109$ m for adiabatic release and $D_{N_{isotherm}} = 0.098$ m for “isothermal” release. The density of ambient air was calculated assuming the ambient temperature $T_a = 283$ K and normal pressure $p_a = 101{,}325$ Pa as $\rho_a = 1.25$ kg/m$^3$. Hydrogen density in the nozzle $\rho_N$ is shown in Table 1 and Table 2 for adiabatic and “isothermal” release respectively.

The outflow conditions changed from sonic to subsonic when the ratio of storage pressure $p_s$ to ambient pressure ratio $p_a$ decreased below the threshold value $\rho_s/\rho_a = 1.9$ bar. For simulated adiabatic blowdown, it happened at $t = 73.3$ s and for “isothermal” blowdown onset of subsonic release conditions occured at $t = 75$ s. The parameter $(\rho_N/\rho_a)(U_N/C_N)^3$ remained above 0.07 and the flame length was calculated as:

$$L_f = 805\left[\left(\frac{\rho_N}{\rho_a}\right)\left(\frac{U_N}{C_N}\right)^3\right]^{0.47} D_N. \tag{3}$$

Figure 5 shows hydrogen flame length as a function of time calculated using both adiabatic and “isothermal” models. Though the flame length may be calculated starting from time $t = 0$ s (and this trend is shown in Fig.5), its comparison with the experiment is meaningful only starting from time $t = 6$ s when the experimental flame established itself and reached maximum length (getting out of the soil). In Fig.2 the experimental flame length at $t = 6$ s is 92 m in Test 1 and 88 m in Test 2. The simulated flame length at $t = 6$ s in the adiabatic release is 119.9 m, which makes a 30% and 36% difference with Test 1 and Test 2 respectively. The simulated flame length in the “isothermal” release is 110.2 m, which is a 20% and 25% difference between Test 1 and Test 2 respectively. Given the dimensionless flame length correlation (1) is conservative by design and expected to wittingly overpredict the experimental data this difference should be considered as acceptable. However, when compared with the longest flame length 111 m reported in [4] the absolute differences are even smaller: merely 7.5% for adiabatic release and -0.7% for isothermal release.

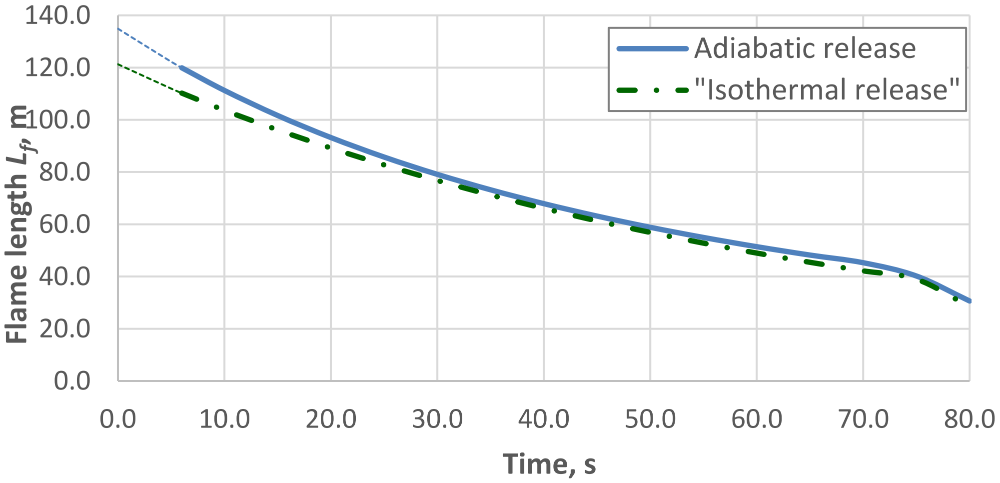

Figure 5. The simulated flame length from full-bore pipe rupture experiments [4].

Table 1. Simulated hydrogen release properties and flame length during adiabatic blowdown.

| Time, s | $p_s$, bar | $T_s$, K | $m_s$, kg | $\rho_N$, kg/m$^3$ | $T_N$, K | $\dot{m}_{H2}$, kg/s | $\rho_N/\rho_a$ | $L_f/D_{N_{ad}}$ | $L_f$, m |
|---|---|---|---|---|---|---|---|---|---|
| 0.0 | 60.0 | 283 | 806.1 | 3.12 | 233.4 | 34.7 | 2.50 | 1237.4 | 134.9 |
| 5.0 | 44.2 | 259 | 653.0 | 2.53 | 214.0 | 26.8 | 2.02 | 1121.4 | 122.2 |
| 6.0 | 41.6 | 254 | 626.8 | 2.43 | 210.4 | 25.5 | 1.94 | 1100.2 | 119.9 |
| 10.0 | 33.0 | 238 | 534.0 | 2.07 | 197.1 | 21.0 | 1.66 | 1020.7 | 111.3 |
| 15.0 | 25.0 | 219 | 440.4 | 1.71 | 182.1 | 16.6 | 1.37 | 932.6 | 101.7 |
| 20.0 | 19.2 | 203 | 366.0 | 1.42 | 168.8 | 13.3 | 1.14 | 855.2 | 93.2 |
| 25.0 | 14.9 | 189 | 306.3 | 1.19 | 157.0 | 10.7 | 0.95 | 786.7 | 85.7 |
| 30.0 | 11.7 | 176 | 258.0 | 1.00 | 146.4 | 8.7 | 0.80 | 725.9 | 79.1 |
| 35.0 | 9.2 | 164 | 218.6 | 0.85 | 136.9 | 7.1 | 0.68 | 671.6 | 73.2 |
| 40.0 | 7.3 | 154 | 186.3 | 0.72 | 128.2 | 5.9 | 0.58 | 623.0 | 67.9 |
| 45.0 | 5.9 | 145 | 159.6 | 0.62 | 120.4 | 4.9 | 0.50 | 579.3 | 63.1 |
| 50.0 | 4.8 | 136 | 137.3 | 0.53 | 113.3 | 4.1 | 0.43 | 539.9 | 58.8 |
| 55.0 | 3.9 | 128 | 118.7 | 0.46 | 106.8 | 3.4 | 0.37 | 504.2 | 55.0 |
| 60.0 | 3.2 | 121 | 103.1 | 0.40 | 100.8 | 2.9 | 0.32 | 471.8 | 51.4 |
| 65.0 | 2.6 | 114 | 89.8 | 0.35 | 95.3 | 2.4 | 0.28 | 442.3 | 48.2 |
| 70.0 | 2.2 | 108 | 78.6 | 0.31 | 90.3 | 2.1 | 0.24 | 415.4 | 45.3 |
| 75.0 | 1.8 | 103 | 69.0 | 0.28 | 87.3 | 1.8 | 0.19 | 368.8 | 40.2 |
| 80.0 | 1.5 | 98 | 61.0 | 0.28 | 87.3 | 1.5 | 0.11 | 281.0 | 30.6 |

Notes: $p_s$ is the storage pressure, $T_s$ is the storage temperature, $m_s$ is the hydrogen mass in storage, $\rho_N$ is the nozzle density, $\rho_a = 1.25$ kg/m$^3$ is the ambient air density, $T_N$ is the temperature in the nozzle, $\dot{m}_{H2}$ is the hydrogen mass flow rate, $D_{N_{ad}}$ is the nozzle diameter in the adiabatic model.

Table 2. Simulated hydrogen release properties and flame length during “isothermal” blowdown.

| Time, s | $p_s$, bar | $T_s$, K | $m_s$, kg | $\rho_N$, kg/m$^3$ | $T_N$, K | $\dot{m}_{H2}$, kg/s | $\rho_N/\rho_a$ | $L_f/D_{N_{isoterm}}$ | $L_f$, m |
|---|---|---|---|---|---|---|---|---|---|
| 0 | 60.0 | 283 | 806.1 | 3.12 | 233.4 | 28.0 | 2.50 | 1237.4 | 121.3 |
| 5 | 46.8 | 263 | 679.5 | 2.63 | 217.5 | 22.7 | 2.11 | 1142.4 | 112.0 |
| 6 | 44.6 | 259 | 657.1 | 2.54 | 214.6 | 21.8 | 2.04 | 1124.7 | 110.2 |
| 10 | 36.9 | 245 | 576.3 | 2.23 | 203.3 | 18.6 | 1.79 | 1057.8 | 103.7 |
| 15 | 29.2 | 243 | 490.8 | 1.90 | 201.1 | 15.7 | 1.52 | 981.1 | 96.2 |
| 20 | 23.2 | 243 | 418.1 | 1.62 | 201.2 | 13.4 | 1.30 | 910.2 | 89.2 |
| 25 | 18.5 | 243 | 356.2 | 1.38 | 201.3 | 11.4 | 1.11 | 844.4 | 82.7 |
| 30 | 14.7 | 243 | 303.6 | 1.18 | 201.5 | 9.7 | 0.94 | 783.4 | 76.8 |
| 35 | 11.7 | 243 | 258.7 | 1.01 | 201.5 | 8.3 | 0.80 | 726.8 | 71.2 |
| 40 | 9.3 | 243 | 220.5 | 0.86 | 201.6 | 7.0 | 0.69 | 674.3 | 66.1 |
| 45 | 7.4 | 243 | 188.0 | 0.73 | 201.7 | 6.0 | 0.58 | 625.7 | 61.3 |
| 50 | 5.9 | 243 | 160.3 | 0.62 | 201.8 | 5.1 | 0.50 | 580.5 | 56.9 |
| 55 | 4.7 | 243 | 136.7 | 0.53 | 201.8 | 4.4 | 0.43 | 538.6 | 52.8 |
| 60 | 3.8 | 243 | 116.5 | 0.45 | 201.8 | 3.7 | 0.36 | 499.8 | 49.0 |
| 65 | 3.0 | 243 | 99.4 | 0.39 | 201.9 | 3.2 | 0.31 | 463.8 | 45.4 |
| 70 | 2.4 | 243 | 84.7 | 0.33 | 201.9 | 2.7 | 0.26 | 430.3 | 42.2 |
| 75 | 1.9 | 243 | 72.3 | 0.28 | 201.9 | 2.3 | 0.22 | 397.7 | 39.1 |
| 80 | 1.5 | 243 | 61.7 | 0.28 | 215.2 | 1.9 | 0.11 | 290.2 | 28.4 |

Notes: $D_{N_{isoterm}}$ is the nozzle diameter in “isothermal” simulations.

## 4.0 CONCLUSIONS

The paper rigorously analyses hydrogen flame length during blowdown from 163 $m^3$ pipeline system at 60 bar through a full-bore ruptured 6” pipeline. Two blowdown models are used to simulate the blowdown process: adiabatic model, neglecting heat exchange and allowing storage temperature decrease to 98 K, and “isothermal” model, which prohibits such strong temperature decrease due to heat transfer from the surroundings through the pipe system walls. The adiabatic blowdown model provided agreement with the described experimental pressure dynamics with the discharge coefficient $C_D = 0.26$. The “isothermal” model with the lower temperature limit of 243 K has demonstrated agreement with experiment with the discharge coefficient $C_D = 0.21$.

The paper originality is in application for the first time of the dimensionless hydrogen flame length correlation by Molkov and Saffers (2013) for analysis of the jet flame resulting from a catastrophic full-bore 6” pipe rupture. The “isothermal” blowdown model, which appears more suitable for the considered experiment with long pipework, provided a particularly good agreement with the experimental observations. The difference between the simulated flame length and the longest experimental flames after the period of the flame establishment ($t = 6$ s) ranges from only -0.7% to 7.5%.

The significance of the performed research is in development of methodology suitable for the analysis of blowdown of large hydrogen storage systems with developed pipeworks and assessment of hydrogen jet flames. This is particularly remarkable that a close agreement between simulated and experimental flame lengths was observed despite the difference between the layout assumed in the model, i.e. release through an orifice in a tank, and the actual experimental conditions, i.e. release towards each other from two cross-sections of a ruptured pipeline.

## 5.0 REFERENCES

1. Astbury, G.R., Hawksworth, S.J. Spontaneous ignition of hydrogen leaks: a review of postulated mechanisms, *Int. J. Hydrogen Energy*, **32**, pp. 2178-2185, 2007.
2. Molkov, V., Saffers, J. B. Hydrogen Jet Flames, *Int. J. Hydrogen Energy*, **38**, No.19, pp. 8141-8158, 2013.
3. Bradley, D., Gaskell, P., Gu, X., Palacios, A. Jet flame heights, lift-off distances, and mean flame surface density for extensive ranges of fuels and flow rates, Combustion and Flames, **164**, pp.400-409, 2016.
4. Acton, M. R., Allason, D., Creitz, L. W., Lowesmith, B. J. Large Scale Experiments to Study Hydrogen Pipeline Fires, 8th International Pipeline Conference, American Society of Mechanical Engineers, Calgary, Alberta, Canada, 2010, pp. 593-602.
5. Molkov, V., Makarov, D., Bragin, M. Physics and modelling of underexpanded jets and hydrogen dispersion in atmosphere, In: Physics of Extreme States of Matter - 2009 (pp. 146-149). Russian Academy of Sciences.
6. Molkov, V. Fundamentals of Hydrogen Safety, 2012, https://bookboon.com (assessed 25 April 2021).
7. https://fch2edu.eu/home/e-laboratory/ (assessed 25 April 2021).
8. Schefer, R.W., Houf, W.G., Williams, T.C., Bourne, B., Colton, J. Characterization of high-pressure, underexpanded hydrogen-jet flames, *Int. J. Hydrogen Energy*, **32**, pp. 2081 – 2093, 2007.